Earthquakes and Structures, *Vol. 7, No. 5 (2014) 817-842*
DOI: http://dx.doi.org/10.12989/eas.2014.7.5.817

Nonlinear modeling parameters of RC coupling beams in a coupled wall system

Seongwoo Gwon[1], Myoungsu Shin[*1], Benjamin Pimentel[2] and Deokjung Lee[3]

[1]*School of Urban and Environmental Engineering, Ulsan National Institute of Science and Technology (UNIST), Ulsan, Korea*
[2]*Rosenwasser Grossman Consulting Engineers, 485 Seventh Avenue, New York, NY, USA*
[3]*Interdisciplinary School of Green Energy, Ulsan National Institute of Science and Technology (UNIST), Ulsan, Korea*

(Received June 7, 2014, Revised September 10, 2014, Accepted September 27, 2014)

Abstract. ASCE/SEI 41-13 provides modeling parameters and numerical acceptance criteria for various types of members that are useful for evaluating the seismic performance of reinforced concrete (RC) building structures. To accurately evaluate the global performance of a coupled wall system, it is crucial to first properly define the component behaviors (i.e., force-displacement relationships of shear walls and coupling beams). However, only a few studies have investigated on the modeling of RC coupling beams subjected to earthquake loading to date. The main objective of this study is to assess the reliability of ASCE 41-13 modeling parameters specified for RC coupling beams with various design details, based on a database compiling almost all coupling beam tests available worldwide. Several recently developed coupling beam models are also reviewed. Finally, a rational method is proposed for determining the chord yield rotation of RC coupling beams.

Keywords: ASCE/SEI 41-13; modeling parameters; coupling beam; chord yield rotation

1. Introduction

Reinforced concrete (RC) structural walls in tall buildings often have vertically aligned consecutive openings, so that the coupling beams have a key role to structurally connect together the wall segments at the floor levels. Coupling beams designed according to current codes (ACI 318-11, ICC 2012, Eurocode 8, CAN/CSA A23.3-04, NZS 3101-1) are expected to have significant inelastic deformations under design-level earthquakes. Adequately designed coupling beams will not only survive over large displacement demands, but also function as energy dissipation devices (Paulay and Priestley 1992). Many previous studies on RC coupling beams (Paulay 1971, Tassios *et al*. 1996, Galano and Vignoli 2000, Yun *et al*. 2008) concentrated on developing the reinforcing layouts to ensure the satisfactory seismic performance.

The performance of coupling beams has a great influence on the overall response of a coupled wall system subjected to earthquake loading (Paulay and Priestley 1992). To accurately evaluate

*Corresponding author, msshin@unist.ac.kr

http://www.techno-press.org/?journal=eas&subpage=7 ISSN: 2092-7614 (Print), 2092-7622 (Online)

Table 1 Modeling parameters for coupling beams in ASCE 41-13

Reinforcement Configuration	$\frac{V_u}{bh\sqrt{f_c'}}$	Group No.	Flexure dominated			Group No.	Shear dominated		
			a	b	c		d	e	c
Conforming transverse reinforcement	≤0.25	1	0.025	0.05	0.75	6	0.02	0.03	0.6
	-	1-2	Linear interpolation			6-7	Linear interpolation		
	≥0.5	2	0.02	0.04	0.5	7	0.016	0.024	0.3
Nonconforming transverse reinforcement	≤0.25	3	0.02	0.035	0.5	8	0.012	0.025	0.4
	-	3-4	Linear interpolation			8-9	Linear interpolation		
	≥0.5	4	0.01	0.025	0.25	9	0.008	0.014	0.2
Diagonal reinforcement	n.a.	5	0.03	0.05	0.8	-	-	-	-

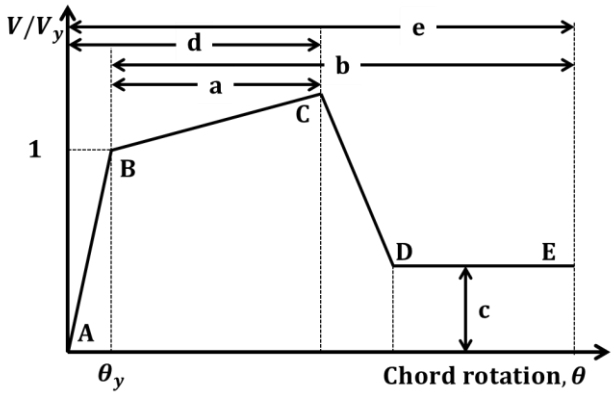

Fig. 1 Idealized modeling backbone curve in ASCE 41-13

the global performance of a coupled wall system, it is crucial to first properly define the component behaviors, i.e., force-displacement relationships of shear walls and associated components such as coupling beams. According to ASCE 7-10, Section 16.2, the numerical model used for nonlinear response history analysis must account for significant hysteretic behaviors of elements consistent with suitable laboratory test data, including yielding, strength degradation, stiffness degradation, and hysteretic pinching. Several documents such as ASCE/SEI 41-13 (ASCE 41-13 hereafter) and ACI 369R-11 provide seismic modeling parameters and numerical acceptance criteria for various types of members including RC coupling beams (see Fig. 1 and Table 1), as well as nonlinear analysis procedures. These standards help engineers to make use of performance-based earthquake engineering for the evaluation of existing buildings or for the design of new buildings.

However, the ASCE 41-13 modeling procedures for RC coupling beams have not been validated enough based on physical test results. Only a few researchers (Ihtiyar and Breña 2006, Ihtiyar and Breña 2007, Brena *et al*. 2009, Naish *et al*. 2013, Wallace 2012) have investigated on

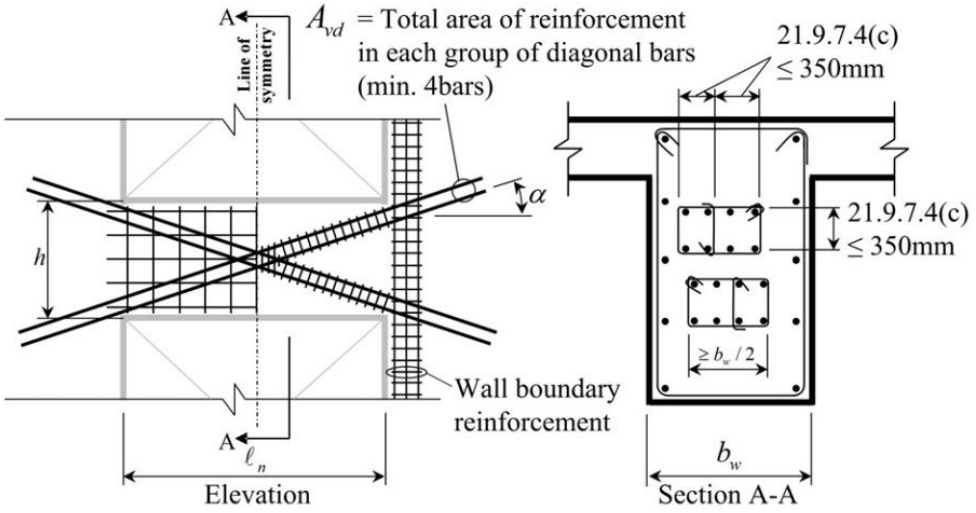

(a) Confinement of individual diagonals

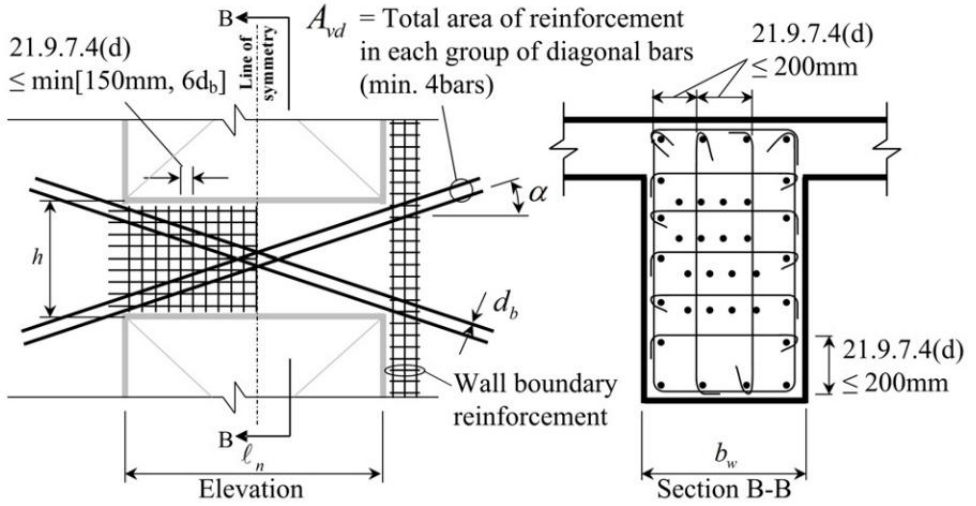

(b) Full confinement of beam section

Fig. 2 Design details for diagonally reinforced coupling beams in ACI 318-11

the modeling of RC coupling beams subjected to seismic loading to date. Given the concern, the main objective of this study is to assess the appropriateness of the ASCE 41-13 modeling parameters for the shear force-chord rotation behaviors of RC coupling beams with various design details. A database of almost all available conventionally and diagonally reinforced coupling beam tests worldwide (Tassios *et al*. 1996, Galano and Vignoli 2000, Yun *et al*. 2008, Ihtiyar and Brena 2007, Barney 1980, Hong and Jang 2006, Paulay and Binney 1974, Lequesne *et al*. 2010, Canbolat *et al*. 2005, Shimazaki 2004) is compiled and used for the assessment. Several recently developed models (Brena *et al*. 2009, Hindi and Hassan 2007) are also reviewed. Finally, a rational method is proposed for determining the chord yield rotation of RC coupling beams.

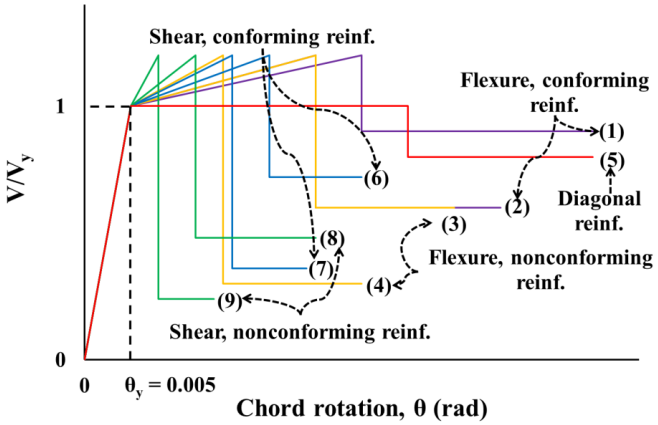

Fig. 3 Schematic modeling backbone curves per ASCE 41-13

2. Factors affecting nonlinear behavior of coupling beams

In this section, several key factors that are considered in ASCE 41-13 to affect the nonlinear force-deformation behavior of RC coupling beams are examined, which include the governing failure mode, longitudinal reinforcement layout, detail of transverse reinforcement, and shear stress level. Also, the ASCE 41-13 procedures to determine the idealized shear force-chord rotation backbone curve of RC coupling beams are reviewed.

2.1 Coupling beam strength

The strength of RC coupling beams can be determined based on the ACI 318 Building Code requirements. The flexural strength of a conventionally reinforced (CR) coupling beam that has main longitudinal bars parallel to the span of the beam is calculated following the procedures in Section 10.2 of ACI 318-11, which are usually used for ordinary slender beams. Then, the beam shear force applied at the event of flexure hinging at both ends of the beam, V_{hinge}, is calculated by:

$$V_{hinge} = \frac{2M_n}{l_n} \tag{1}$$

Here, M_n is the nominal flexural strength of the coupling beam calculated using the anticipated strengths of materials, and l_n is the clear span length of the beam. The nominal shear strength of a CR coupling beam, V_n, is estimated using ACI 318-11 Eq. (21-7):

$$V_n = A_{cv}(\alpha_c\sqrt{f'_c} + \rho_v f_{yt}) \tag{2}$$

The value of α_c varies depending on the span-to-depth ratio l_n/h, where h is the depth of the beam. α_c is equal to 3 if $l_n/h < 1.5$, 2 if $l_n/h > 2$, and is linearly interpolated if l_n/h is between 1.5 and 2. $\rho_v = A_v/(b_w s)$ is the ratio of transverse reinforcement with the spacing of s, b_w is the beam width, and f_{yt} is the yield stress of transverse reinforcement. A_{cv} is the cross-sectional area of the coupling beam. It is noted that Eq. (2) does not account for the shear strength degradation caused by cyclic loading at large displacements.

The strength of diagonally reinforced (DR) coupling beams shown in Fig. 2 is determined based on Section 21.9.7 of ACI 318-11. It is assumed that both the flexural and shear strengths of a DR coupling beam depend only on the contribution of diagonal reinforcement. In other words, the contribution of horizontal reinforcement is not included in the flexural strength. The nominal flexural strength (M_n) of a DR coupling beam is calculated by:

$$M_n = A_s f_y \cos\alpha \, (h - 2d') \tag{3}$$

Also, the effects of concrete and transverse reinforcement on the shear strength of DR coupling beams are not considered in ACI 318-11. The nominal shear strength (V_n) of a DR coupling beam is expressed as follows:

$$V_n = 2A_s f_y \sin\alpha \tag{4}$$

Here, A_s is the total area of diagonal reinforcement in one direction, and f_y is the yield stress of diagonal reinforcement. Also, h is the depth of the beam, and d' is the distance from the top (or bottom) of the beam to the centroid of diagonal reinforcement. α is the inclination angle between the diagonal bars and the longitudinal axis of the beam (see Fig. 2).

2.2 Failure mode

Some earlier studies were dedicated to investigating the failure modes of RC coupling beams (Paulay 1971, Paulay and Binney 1974). They identified the primary design parameters affecting the failure modes, which include the reinforcement layout, span-to-depth ratio, longitudinal and transverse reinforcement ratios, and shear stress level. In general, a stable nonlinear flexural mechanism is difficult to be achieved in most coupling beams because of their small span-to-depth ratios and shear strength degradation caused by cyclic loading. Paulay (1971) found that conventionally reinforced (CR) coupling beams were vulnerable to shear (diagonal tension) failure even at small deformation levels. Moreover, CR coupling beams having enough transverse reinforcement may still suffer sliding shear failure at the beam ends. In contrast, diagonally reinforced (DR) coupling beams showed much more ductile behaviors than CR coupling beams (Paulay and Binney 1974). A sufficient amount of confinement reinforcement should be provided to prevent the bucking of diagonal bars, but the confinement reinforcement usually causes steel congestion and resulting difficulty during concrete placement. Thus, some recent studies have attempted to relieve steel congestion problems in DR coupling beams by utilizing high performance fiber-reinforced cementitious composites (HPFRCCs) (Lequesne *et al*. 2010, Canbolat *et al*. 2005).

According to ASCE 41-13, the governing failure modes of coupling beams strongly affect the force-deformation backbone curves (Table 1). The governing failure mode of a CR coupling beam is defined as either "flexure-dominated" or "shear-dominated". In the case of DR coupling beams, however, only the flexure-dominated mode is assumed (Table 1). The governing mode of a CR coupling beam is judged by comparing the shear force applied at flexural hinging V_{hinge} with the nominal shear strength V_n, which are calculated following the ACI building code requirements, as discussed in the previous section. When a CR coupling beam is expected to have the shear demand (V_{hinge}) less than the shear capacity (V_n), the coupling beam is considered flexure-dominated. It is considered shear-dominated in the opposite case.

The "a" and "b" parameters in Table 1 represent the chord rotations of a flexure-dominated

coupling beam, while the "d" and "e" parameters are for those of a shear-dominated coupling beam. The "c" parameter stands for the residual strength of a coupling beam at large rotation as a fraction of beam shear force at the yield point. It is noted that the values of "d" and "e" are roughly 20 to 40% less than the values of "a" and "b", respectively (Fig. 3). Also, the value of "c" for a shear-dominated coupling beam is equal to 60 or 80% of that for a flexure-dominated coupling beam (Fig. 3). These reflect that coupling beams controlled by shear generally show smaller ductilities as well as lower residual strengths.

2.3 Transverse reinforcement and shear stress level

Two other factors affecting the selection of the tabulated deformation and strength parameters in Table 1 are transverse reinforcement detail and shear stress level. Note that the two factors are not considered for DR coupling beams, for which the parameter values are assigned to be the largest. To be qualified as "conforming transverse reinforcement" noted in Table 1, two conditions must be satisfied according to ASCE 41-13. First, closed stirrups should be arranged at a spacing less than $d/3$ over the entire span of the coupling beam, where d is the flexural depth. Second, the shear strength of the stirrups V_s should be at least 3/4 of the required shear strength of the coupling beam.

Two discrete values of the shear stress level equal to 0.25 and 0.5 in MPa units (3 and 6 in psi units) are used to classify the deformation and strength parameters in Table 1. The shear stress level τ is calculated by:

$$\tau = \frac{V_u}{bh\sqrt{f'_c}} \tag{5}$$

Here, V_u is the ultimate shear force in the coupling beam, b is the width of the beam, h is the depth of the beam, and f'_c is the concrete compressive strength in MPa or psi (V_u/bh is in MPa or psi). In the case of a CR coupling beam having the shear stress level between 0.25 and 0.5 in MPa units, the deformation and strength parameters are to be interpolated between the tabulated values.

It is noted that the parameter values in Table 1 are the smallest for CR coupling beams with non-conforming transverse reinforcement, subjected to the shear stress level higher than 0.5 in MPa units. This indicates that CR coupling beams in such conditions may suffer premature diagonal tension or sliding shear failure.

2.4 Chord yield rotation

For RC coupling beams having inelastic behavior governed by flexure, the estimation of chord yield rotation θ_y is the first step for constructing the backbone curve of the cyclic load-displacement response under seismic loading. In contrast, the yield point is not defined for coupling beams whose inelastic behavior is governed by shear. ASCE 41-13 requires that the chord yield rotation for a flexure-dominated coupling beam is calculated by:

$$\theta_y = \left(\frac{M_y}{E_c I_{cr}}\right) l_p \tag{6}$$

Here, M_y stands for the yield moment of the coupling beam, I_{cr} is the cracked moment of inertia of the beam section, E_c is the modulus of elasticity of concrete, and l_p is the plastic hinge length. ASCE 41-13 recommends that I_{cr} is taken as one-half of the gross moment of inertia, $0.5I_g$, and l_p

is assumed equal to *d*/2, where d is the effective flexural depth. Also, E_c may be taken equal to $4700\sqrt{f'_c}$ in MPa ($57000\sqrt{f'_c}$ in psi) per ACI 318-11.

After the chord yield rotation is determined, the deformation and strength parameters in Table 1 are used to establish the significant points (B, C, D, and E) in the idealized shear force-chord rotation backbone curve shown in Fig. 1. The deformation and strength parameters of a coupling beam are determined based on the governing failure mode, longitudinal reinforcement layout, transverse reinforcement detail, and shear stress level.

3. Review for recent coupling beam models

An accurate calculation for the chord yield rotation of a coupling beam is crucial for modeling the load-deformation backbone curve based on ASCE 41-13. However, it is known that the ASCE 41-13 method using Eq. (6) generally underestimates the chord yield rotation compared with the test results. Recently, several researchers have attempted to better estimate the nonlinear load-deformation response of RC coupling beams under lateral loading. This section reviews the recently proposed models.

3.1 Chord yield rotation formula by Ihtiyar and Brena (2007)

ASCE 41-13 specifies that the chord yield rotation of a coupling beam is calculated by using the cracked moment of inertia equal to one-half of the gross moment of inertia. Paulay and Priestley (1992) proposed more detailed formulas for the cracked moment of inertia that take into account the length-to-depth aspect ratio of coupling beams. They defined the cracked moment of inertia (I_{cr}) as:

$$I_{cr} = \frac{0.2I_g}{\left[1+3\left(\frac{h}{l_n}\right)^2\right]} \text{ for conventionally reinforced coupling beams} \quad (7)$$

$$I_{cr} = \frac{0.4I_g}{\left[1+3\left(\frac{h}{l_n}\right)^2\right]} \text{ for diagonally reinforced coupling beams} \quad (8)$$

These equations also tend to underestimate the chord yield rotation when they are used in conjunction with Eq. (6), although they give better estimates than ASCE 41-13. The discrepancy between the measured and calculated chord yield rotations likely happens because Eq. (6) only considers the contribution of flexural deformation on the chord rotation and does not account for the effect of shear deformation or reinforcing bar bond slip.

The total chord yield rotation, θ_y, of a coupling beam may be separated into the chord rotation due to flexural deformation, θ_{yf}, and the chord rotation due to shear deformation, θ_{yv}:

$$\theta_y = \theta_{yf} + \theta_{yv} \quad (9)$$

The shear deformation component, θ_{yv}, may be calculated by dividing the beam shear force at yield, V_y, by the effective shear stiffness, GA_v:

$$\theta_{yv} = \frac{V_y}{(GA_v/K_v)} \tag{10}$$

Here, A_v is the effective shear area, taken equal to the gross section area (A_g) divided by 1.2 for a rectangular section, and G is the shear modulus of concrete. The constant K_v is used to consider the degradation of shear stiffness by cyclic loading.

Ihtiyar and Brena (2007) tested four conventionally reinforced coupling beams, and compared the shear force-chord rotation responses from the tests with the backbone curves determined following the ASCE 41-13 procedures. Based on the results, they proposed a new formula for the chord yield rotation that takes into account the shear deformation and the shear stiffness degradation by cyclic loading as follows:

$$\theta_{y\_Brena} = \left(\frac{M_y}{E_c I_{mod}}\right) l_p + \frac{V_y}{(GA_v/K_v)} \tag{11}$$

Here, I_{mod} is to be estimated using Eq. (12). Later, Ihtiyar and Brena (2007) suggested using the modification to the cracked moment of inertia that Paulay and Priestly (1992) proposed to address the effect of reinforcing bar bond slip in structural walls:

$$I_{mod} = \frac{I_{cr}}{1.2 + \frac{30 I_{cr}}{l_n^2 bh}} \tag{12}$$

I_{mod} is the modified cracked moment of inertia that takes into account the chord rotation due to reinforcing bar slippage at coupling beam-wall interfaces. This equation is to be used with Eq. (11) to calculate the chord yield rotation.

3.2 Coupling beam truss model by hindi and hassan (2007)

Hindi and Hassan (2007) employed a simple truss model to examine the nonlinear force-resisting mechanism of diagonally reinforced coupling beams. In the truss model, it is supposed that all forces are resisted by a pair of diagonal tension tie and diagonal compression strut (Fig. 4), and that the diagonal tension is carried only by diagonal reinforcement. However, the diagonal compression is deemed to be carried by a combination of diagonal reinforcement and concrete core surrounded by the diagonal reinforcement (Fig. 4).

Presuming that the diagonal tensile and compressive forces (T and C) are constant along the beam span, they are computed by:

$$T = A_s^+ f_s^+ = A_s^+ f_s(\varepsilon_s^+) \tag{13}$$

$$C = A_s^- f_s^- + A_c f_c^- = A_s^- f_s(\varepsilon_s^-) + A_c f_c(\varepsilon_c^-) \tag{14}$$

Here, A_s is the area of diagonal reinforcement, A_c is the concrete core area confined by diagonal reinforcement in compression, f_c and f_s are the concrete and steel stresses, and ε_c and ε_s are the concrete and steel strains in the diagonal directions, respectively. Note that the superscripts "+" and "-" stand for tensile and compressive properties, respectively. The total shear force, V, in a diagonally reinforced coupling beam is taken as:

$$V = (T + C)\sin\alpha \tag{15}$$

Here, α is the inclination angle of diagonal reinforcement, as shown in Fig. 4.

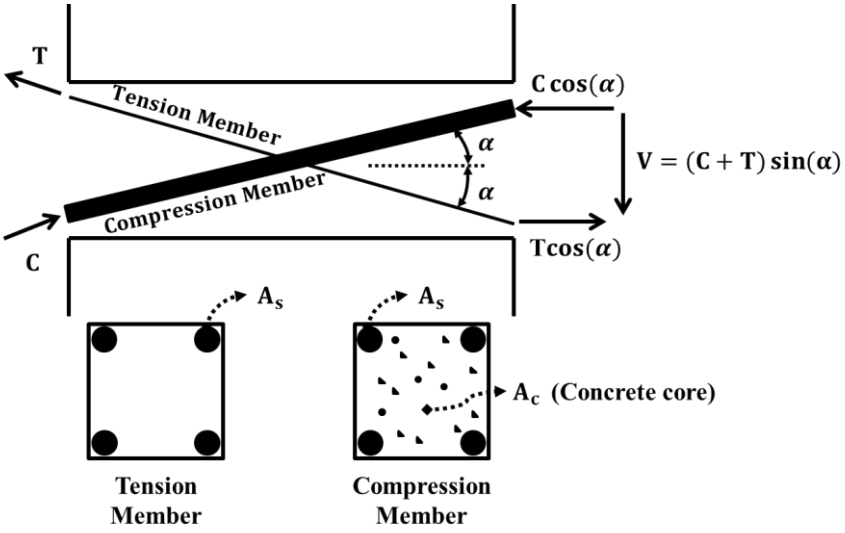

Fig. 4 Truss model by Hindi and Hassan (2007)

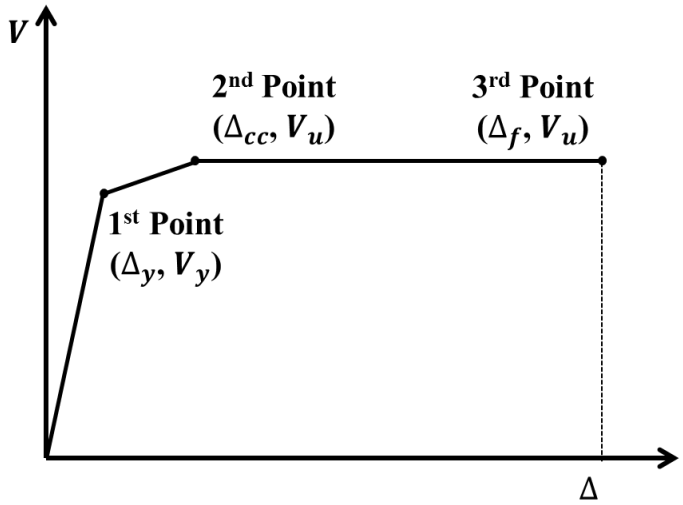

Fig. 5 Key points of trilinear approximation method by Hindi and Hassan (2007)

In this model, it is assumed that the bond between concrete and reinforcement is perfect, and the strains in the two diagonal directions in Fig. 4 are the same in magnitude ($\varepsilon_s^+ = \varepsilon_s^- = \varepsilon_c^- = \varepsilon$). Therefore, the lateral displacement of one end to the other end of a coupling beam, Δ, can be described as:

$$\Delta = \varepsilon \frac{L}{\cos\alpha \sin\alpha} \tag{16}$$

Here, L is the span length of the coupling beam and ε is the strain in the diagonal directions. Then,

the chord rotation of the coupling beam is given by $\theta = \Delta/L$. Using Eqs. (13) to (16), the shear force V and the lateral displacement Δ in a diagonally reinforced coupling beam can be determined at any given diagonal strain ε.

On the practical viewpoint, Hindi and Hassan (2007) proposed a simplified trilinear model for the force-displacement backbone response of diagonally reinforced coupling beams subjected to cyclic loading, as shown in Fig. 5. The first critical point in the simplified trilinear curve is defined at the yield point of diagonal reinforcement, when the diagonal strain is equal to the yield strain of the reinforcement: $\varepsilon = \varepsilon_y$. The concrete core is assumed to reach the unconfined compressive strength f'_c at the same time. Thus, the beam shear force at this yield point is computed by:

$$V_y = (T_y + C_y)\sin\alpha \tag{17}$$

$$T_y = A_s f_y \tag{18}$$

$$C_y = A_s f_y + A_c(f'_c) \tag{19}$$

Here, T_y and C_y are the diagonal tensile and compressive forces at the yield point respectively, f_y is the yield stress of the diagonal reinforcement, and f'_c is the unconfined compressive strength of the concrete. The lateral displacement at the yield point, Δ_y, is expressed as:

$$\Delta_y = \varepsilon_y \frac{L}{\cos\alpha \sin\alpha} \tag{20}$$

After the concrete core reaching its unconfined compressive strength f'_c, it will take additional compressive force until the stress increases to the confined compressive strength f'_{cc} at a strain of ε'_{cc}, as proposed by Mander *et al.* (1988). This is attributed to the confinement by the diagonal reinforcement (Fig. 6). Thus, the diagonal compressive force C_u at this point is computed by:

$$C_u = A_s f_y + A_c f'_{cc} \tag{21}$$

Note that the stress in the diagonal reinforcement remains equal to the yield stress f_y because steel is typically in the perfectly plastic region at a strain of ε'_{cc}. Thus, the beam shear force at this point is determined by:

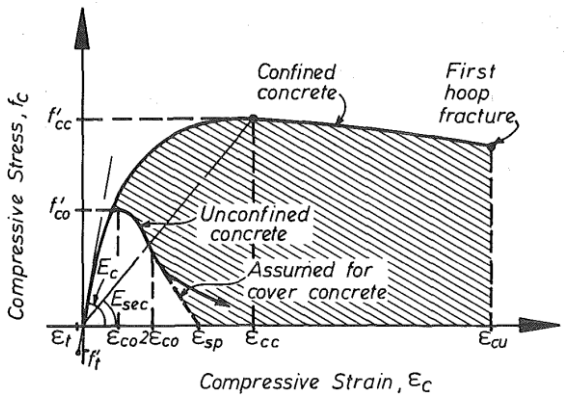

Fig. 6 Mander's concrete confinement model (Mander *et al.* 1988)

$$V_u = (T_y + C_u)\sin\alpha \tag{22}$$

Here, the diagonal tensile force is equal to T_y in Eq. (22). The lateral displacement at this point is estimated by:

$$\Delta_{cc} = \varepsilon'_{cc}\frac{L}{\cos\alpha\sin\alpha} \tag{23}$$

The set of V_u and Δ_{cc} represents the second critical point of the simplified trilinear curve for diagonally reinforced coupling beams (Fig. 5).

To determine the last point of the simplified trilinear curve (Fig. 5), Hindi and Hassan (2007) defined that the failure occurs when the diagonal concrete core crushes (which ultimately results in the buckling of the diagonal reinforcement) or the diagonal reinforcement fractures. Also, they assumed that the shear capacity remains unchanged from V_u defined for the second point. Thus, the lateral displacement at this failure point is computed by:

$$\Delta_f = \varepsilon_f\frac{L}{\cos\alpha\sin\alpha} \tag{24}$$

Here, ε_f is the smaller of the strain at confined concrete crushing (ε_{ccu}) and the strain at steel rupture (ε_{su}). The crushing strain (ε_{ccu}) of the diagonal concrete core is calculated based on Mander *et al*. (1988).

4. Proposed yield stiffness method

From the previous test results in literature, the authors found that shallow coupling beams (Shin *et al*. 2014) generally showed smaller percentages of stiffness reduction than deep coupling beams (Tassios *et al*. 1996, Galano and Vignoli 2000, Yun *et al*. 2008, Ihtiyar and Brena 2007, Wallace 2007) in the essentially elastic range of behavior. This indicates that the length-to-depth ratio has a great impact on the stiffness degradation. It is noted, however, that ASCE 41-13 takes no account of the effect of beam slenderness in estimating the chord yield rotation of a coupling beam.

Also, both shear deformation and shear stiffness degradation could make significant contributions on the lateral displacement of a coupling beam, as discussed earlier. This is especially so when the length-to-depth ratio is small. Ihtiyar and Brena (2007) proposed a chord yield rotation formula considering such contributions in Eq. (11). However, their model appears to be somewhat irrational in the point that the flexural and shear force-deformation relationships are formulated in a completely decoupled arrangement.

In this study, a more rational method is proposed to take into account the effects of shear deformation as well as shear stiffness degradation on the chord yield rotation of coupling beams. The proposed method is based on Timoshenko's beam theory (Cowper 1966) Assuming that the wall edges linked by a coupling beam remain parallel after deformation under lateral loading (i.e., no relative rotation occurs between the beam ends), the yield stiffness $K_{y,cal}$ of a coupling beam may be assessed by:

$$K_{y,cal} = \frac{12E_cI_{mod}}{(1+\Phi_y)l^3},\ \Phi_y = \frac{12E_cI_{mod}}{(0.1G_cA_v)l^2} \tag{25}$$

Table 2 Database of 20 conventionally reinforced coupling beam tests

Specimen		b (mm)	h (mm)	l/h	Longitudinal steel		f_{cm} (MPa)	P_{max} (kN)	$P_{n,0}$ (kN)	$\frac{P_{max}}{P_{n,0}}$
Author	Name				A_s (mm^2)	f_y (MPa)				
Galano & Vignoli (2000)	P01	150	400	1.50	314	567	48.9	224	211	1.06
	P02	150	400	1.50	314	567	44.5	232	211	1.10
Ihtiyar & Brena (2007)	CB-1	250	380	1.34	600	517	39.0	480	492	0.98
	CB-2	250	380	2.68	851	448	39.0	275	187	1.47
	CB-3	250	380	1.34	860	517	31.0	506	575	0.88
	CB-4	250	380	2.68	400	517	30.0	240	205	1.17
Hong & Jang (2006)	01MCB16-SMM	150	480	1.67	398	475	28.7	247	196	1.26
	02MCB13-SMM	150	600	1.33	398	475	28.7	344	253	1.36
	03MCB20-SMM	150	400	2.00	398	475	28.7	219	158	1.39
	07MCB16-SLM	150	480	1.67	398	475	28.7	260	196	1.33
	08MCB16-SHM	150	480	1.67	398	475	28.7	244	196	1.24
	10MCB16-SMN	150	480	1.67	398	475	28.7	213	196	1.09
Bristowe (2000)	NR2	300	500	3.60	1530	433	41.0	321	306	1.05
	NR4	300	500	3.60	1530	433	41.0	321	306	1.05
	MR2	300	500	3.60	1530	433	79.8	328	318	1.03
	MR4	300	500	3.60	1530	433	79.8	328	318	1.03
Barney *et al.* (2000)	C2	102	169	2.50	128	516	21.0	46	57	0.81
	C5	102	169	2.50	128	457	21.7	42	51	0.82
	C7	102	169	5.00	128	459	25.6	23	25	0.92
Yun *et al.* (2008)	CB-3 (*)	200	600	1.00	402	474	57.0	785	398	1.97
(*): Specimens with axial restraint								Average		1.15
								Standard dev.		0.27

$$E_c = 4700\sqrt{f_c'}\,,\ G_c = 0.4E_c \tag{26}$$

Here, E_c is the modulus of elasticity of concrete in MPa, specified in ACI 318-11 1, I_{mod} is the modified cracked moment of inertia of the beam section suggested by Ihtiyar and Brena (2007), l is the length of the coupling beam, and Φ_y is a factor accounting for the relative importance of shear deformation to flexural deformation at the yield point. Also, G_c is the shear modulus of concrete, and A_v is the effective shear area, taken equal to A_g/1.2 for a rectangular section. Eq. (25) stands for the stiffness against the translation lateral to the axis of the coupling beam with no relative rotation between the beam ends.

Table 3 Database of 27 diagonally reinforced coupling beam tests

Specimen		b (mm)	h (mm)	l/h	Diagonal steel		α (°)	f_{cm} (MPa)	P_{max} (kN)	$P_{n,0}$ (kN)	$\frac{P_{max}}{P_{n,0}}$
Author	Name				A_{vd} (mm^2)	f_y (MPa)					
Tassios *et al*. (1996)	CB-2A	130	500	1.00	314	504	39.0	28.5	283	215	1.32
	CB-2B	130	300	1.67	314	504	23.0	26.3	170	147	1.16
Galano 3 Vignoli (2000)	P05	150	400	1.50	314	567	28.5	39.9	239	199	1.20
	P07	150	400	1.50	314	567	28.5	54.0	238	199	1.20
	P08	150	400	1.50	314	567	28.5	53.4	238	199	1.20
	P10	150	400	1.50	314	567	28.5	46.8	241	199	1.21
	P11	150	400	1.50	314	567	28.5	39.9	239	199	1.20
	P12	150	400	1.50	314	567	28.5	41.6	240	199	1.21
Canbolat *et al*. (2005)	Spec. 3	150	600	1.00	398	450	36.0	57.0	800	582	1.37
Paulay & Binney (1974)	317	152	787	1.29	1548	280	33.0	50.7	600	525	1.14
	395	152	991	1.03	1548	265	41.0	35.5	650	530	1.23
Shimazaki (2004)	N1	200	400	2.50	804	476	17.5	54.0	351	365	0.96
	N2	200	400	2.50	804	459	17.5	51.0	400	352	1.14
	N3	200	400	2.50	804	476	17.5	54.0	351	365	0.96
	N4	200	400	2.50	804	459	17.5	51.0	400	352	1.14
	N5	200	400	2.50	804	459	17.5	51.0	393	352	1.12
	N6	200	400	2.50	804	386	17.5	64.0	347	310	1.12
	N7	200	400	2.50	1134	380	17.5	48.0	380	387	0.98
	N8	200	400	2.50	804	383	17.5	32.0	331	313	1.06
Barney *et al*. (1980)	C6	102	169	2.50	142	488	27.5	18.1	60	64	0.93
Lequesne *et al*. (2010)	CB-1 (*)	150	600	1.75	402	430	24.0	45.0	660	465	1.42
	CB-2 (*)	150	600	1.75	402	430	24.0	32.0	655	400	1.64
	CB-3 (*)	150	600	1.75	402	420	24.0	34.0	650	435	1.49
Yun *et al*. (2008)	CB-1 (*)	200	600	1.00	398	474	30.0	44.0	704	530	1.33
	CB-2 (*)	200	600	1.00	398	474	30.0	57.0	866	532	1.63
Shin *et al*. (2014)	1DF0Y	250	1050	3.50	2040	478	8.0	29.2	473	270	1.75
	1DF2Y	250	1050	3.50	2040	478	8.0	49.2	533	270	1.97
										Average	1.26
		(*): Specimens with axial restraint								Standard dev.	0.25

Table 4 Comparison of tested and calculated chord yield rotations for CR beams

Specimen		ASCE Group No.	$\theta_{y,exp}$ *(rad)*	$\theta_{y,ASCE}$ *(rad)*	$\theta_{y,Brena}$ *(rad)*	$\theta_{y,prop}$ *(rad)*	$\frac{\theta_{y,exp}}{\theta_{y,ASCE}}$	$\frac{\theta_{y,exp}}{\theta_{y,Brena}}$	$\frac{\theta_{y,exp}}{\theta_{y,prop}}$
Author	Name								
Galano & Vignoli (2000)	P01	2	0.0081	0.0011	0.0092	0.0072	7.4	0.9	1.1
	P02	2	0.0078	0.0012	0.0097	0.0075	6.5	0.8	1.0
Ihtiyar & Brena (2007)	CB-1	2	0.0190	0.0014	0.0124	0.0086	13.6	1.5	2.2
	CB-2	8-9	0.0067	0.0014	0.0076	0.0080	4.8	0.9	0.8
	CB-3	2	0.0211	0.0021	0.0187	0.0132	10.0	1.1	1.6
	CB-4	1-2	0.0093	0.0009	0.0048	0.0079	10.3	1.9	1.2
Hong & Jang (2006)	01MCB16-SMM	2	0.0089	0.0014	0.0104	0.0085	6.4	0.9	1.0
	02MCB13-SMM	2	0.0092	0.0012	0.0112	0.0080	7.7	0.8	1.2
	03MCB20-SMM	2	0.0124	0.0015	0.0100	0.0090	8.3	1.2	1.4
	07MCB16-SLM	2	0.0104	0.0014	0.0104	0.0085	7.4	1.0	1.2
	08MCB16-SHM	2	0.0105	0.0013	0.0098	0.0081	8.1	1.1	1.3
	10MCB16-SMN	2	0.0083	0.0012	0.0091	0.0071	6.9	0.9	1.2
Bristowe (2000)	NR2	3-4	0.0087	0.0014	0.0067	0.0087	6.2	1.3	1.0
	NR4	1-2	0.0081	0.0014	0.0067	0.0087	5.8	1.2	0.9
	MR2	3	0.0093	0.0011	0.0049	0.0065	8.5	1.9	1.4
	MR4	1	0.0089	0.0011	0.0049	0.0065	8.1	1.8	1.4
Barney *et al*. (2000)	C2	2	0.0064	0.0019	0.0109	0.0135	3.4	0.6	0.5
	C5	1-2	0.0070	0.0017	0.0095	0.0118	4.1	0.7	0.6
	C7	1-2	0.0055	0.0014	0.0058	0.0122	3.9	0.9	0.5
Yun *et al*. (2008)	CB-3 (*)	2	0.0121	0.0004	0.0057	0.0046	30.3	2.1	2.6
*: Specimens with axial restraint					Average		8.38	1.18	1.21
					Standard dev.		5.67	0.45	0.52

In Eq. (25), the effect of shear deformation is accounted by the factor Φ_y, and the effect of shear stiffness degradation due to cyclic loading is accounted by the reduced shear stiffness taken equal to 0.1 times G_cA_v. Once the yield stiffness is determined, the chord yield rotation θ_y can be estimated by dividing the yield moment strength M_y by the yield stiffness $K_{y,cal}$. Modeling backbone curves were generated for compiled coupling beams by applying proposed chord yield rotations. Before applying several modeling techniques, almost available coupling beams data for previous literatures were compiled for analysis (Table 2 and Table 3). Once the proposed chord yield rotations were determined (Table 4 and Table 5), modeling backbone curves were generated in ASCE 41-13 techniques. Those proposed modeling results were compared with test and other modeling methods.

Table 5 Comparison of tested and calculated chord yield rotations for DR beams

Specimen		ASCE Group No.	$\theta_{y,exp}$ *(rad)*	$\theta_{y,ASCE}$ *(rad)*	$\theta_{y,Brena}$ *(rad)*	$\theta_{y,prop}$ *(rad)*	$\frac{\theta_{y,exp}}{\theta_{y,ASCE}}$	$\frac{\theta_{y,exp}}{\theta_{y,Brena}}$	$\frac{\theta_{y,exp}}{\theta_{y,prop}}$
Author	Name								
Tassios *et al*. (1996)	CB-2A		0.0185	0.0011	0.0087	0.0054	16.8	2.1	3.4
	CB-2B		0.0258	0.0016	0.0081	0.0066	16.1	3.2	3.9
Galano & Vignoli (2000)	P05		0.0082	0.0010	0.0059	0.0054	8.2	1.4	1.5
	P07		0.0057	0.0009	0.0051	0.0046	6.3	1.1	1.2
	P08		0.0043	0.0009	0.0051	0.0046	4.8	0.8	0.9
	P10		0.0063	0.0010	0.0054	0.0042	6.3	1.2	1.5
	P11		0.0084	0.0010	0.0059	0.0046	8.4	1.4	1.8
	P12		0.0080	0.0010	0.0058	0.0045	8.0	1.4	1.8
Canbolat *et al*. (2005)	Spec. 3		0.0028	0.0007	0.0053	0.0029	4.0	0.5	1.0
Paulay & Binney (1974)	317		0.0037	0.0004	0.0035	0.0055	9.3	1.1	0.7
	395		0.0038	0.0004	0.0038	0.0067	9.5	1.0	0.6
Shimazaki (2004)	N1	5	0.0059	0.0013	0.0051	0.0050	4.5	1.2	1.2
	N2		0.0059	0.0013	0.0051	0.0050	4.5	1.2	1.2
	N3		0.0060	0.0013	0.0051	0.0050	4.6	1.2	1.2
	N4		0.0061	0.0013	0.0051	0.0050	4.7	1.2	1.2
	N5		0.0059	0.0013	0.0051	0.0050	4.5	1.2	1.2
	N6		0.0068	0.0010	0.0038	0.0037	6.8	1.8	1.8
	N7		0.0065	0.0016	0.0061	0.0060	4.1	1.1	1.1
	N8		0.0063	0.0014	0.0053	0.0052	4.5	1.2	1.2
Barney *et al*. (1980)	C6		0.0060	0.0033	0.0122	0.0025	1.8	0.5	2.4
Lequesne *et al*. (2010)	CB-1 (*)		0.0084	0.0007	0.0034	0.0030	12.0	2.5	2.8
	CB-2 (*)		0.0102	0.0009	0.0040	0.0028	11.3	2.6	3.6
	CB-3 (*)		0.0081	0.0008	0.0038	0.0022	10.1	2.1	3.7
Yun *et al*. (2008)	CB-1 (*)		0.0061	0.0004	0.0033	0.0020	15.3	1.8	3.1
	CB-2 (*)		0.0081	0.0004	0.0029	0.0025	20.3	2.8	3.2
Shin *et al*. (2014)	1DF0Y		0.0151	0.0023	0.0086	0.0111	6.6	1.8	1.4
	1DF2Y		0.0267	0.0023	0.0066	0.0111	11.6	4.0	2.4
*: Specimens with axial restraint					Average		8.33	1.61	1.89
					Standard dev.		4.61	0.82	1.01

5. Reliability assessment of ASCE 41-13 based on test results

Most available coupling beam tests from the literature (Tassios *et al*. 1996, Galano and Vignoli 2000, Yun *et al*. 2008, Ihtiyar and Brena 2007, Barney 1980, Bristowe 2006, Hong and Jang 2006, Paulay and Binney 1974, Lequesne *et al*. 2010, Canbolat *et al*. 2005,

Shimazaki 2004) are compiled in a database to analyze the nonlinear responses of coupling beams subjected to earthquake-type loading. The main test variables of the complied conventionally reinforced (CR) and diagonally reinforced (DR) coupling beams are summarized in Table 2 and Table 3, respectively. The test variables include reinforcement layout, length-to-depth aspect ratio, shear stress level, and concrete compressive strength.

The post-yield deformation capacity of RC coupling beams is investigated using the compiled test database. The ductility of each coupling beam in Tables 2 and 3 is quantified in the shear force-chord rotation response acquired from the test, through dividing the ultimate displacement (or rotation) measured at the point of a 20% strength drop from the maximum load by the yield displacement (or rotation), determined based on Paulay and Priestley (1992) and Kim *et al*. (2012). The experimental ductility values for all the CR coupling beams are plotted in Fig. 7a, with respect to the length-to-depth aspect ratio as well as the shear stress level. Although the ductility data are widely scattered, it is noted that the ductility generally becomes larger as the aspect ratio increases, and it becomes smaller as the shear stress level increases (Fig. 7a). Similar trends are found among the ductility values of the DR coupling beams (Fig. 7b), although the effect of the aspect ratio is less clearly identified.

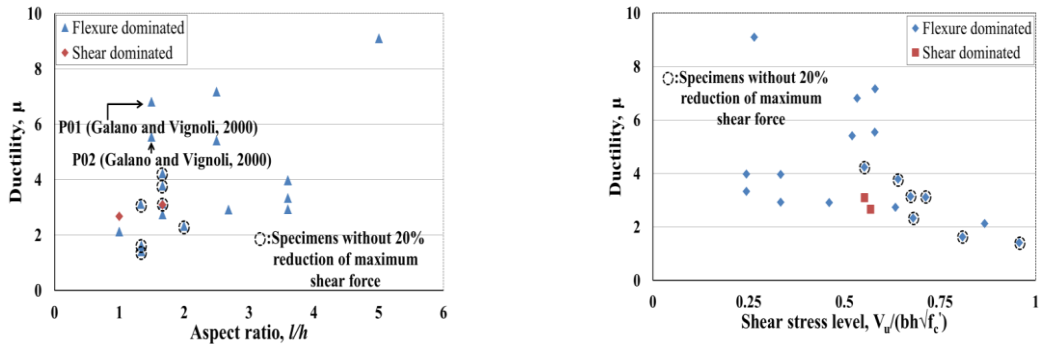

(a) Conventionally reinforced coupling beams

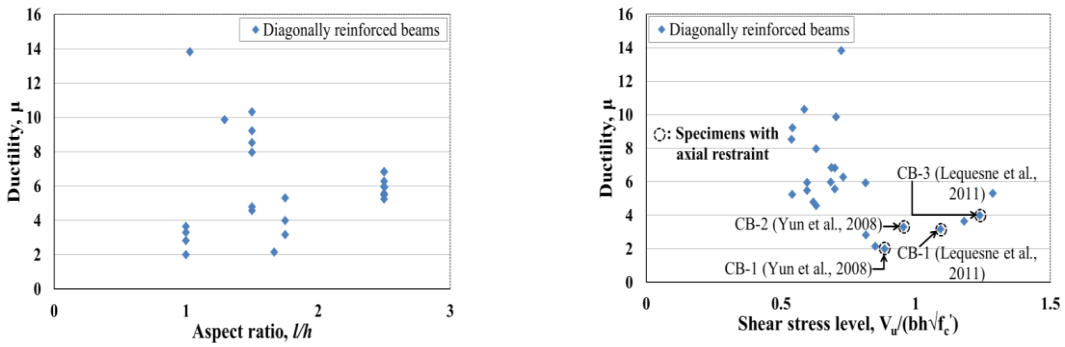

(b) Diagonally reinforced coupling beams

Fig. 7 Effects of length-to-depth aspect ratio and shear stress level on ductility

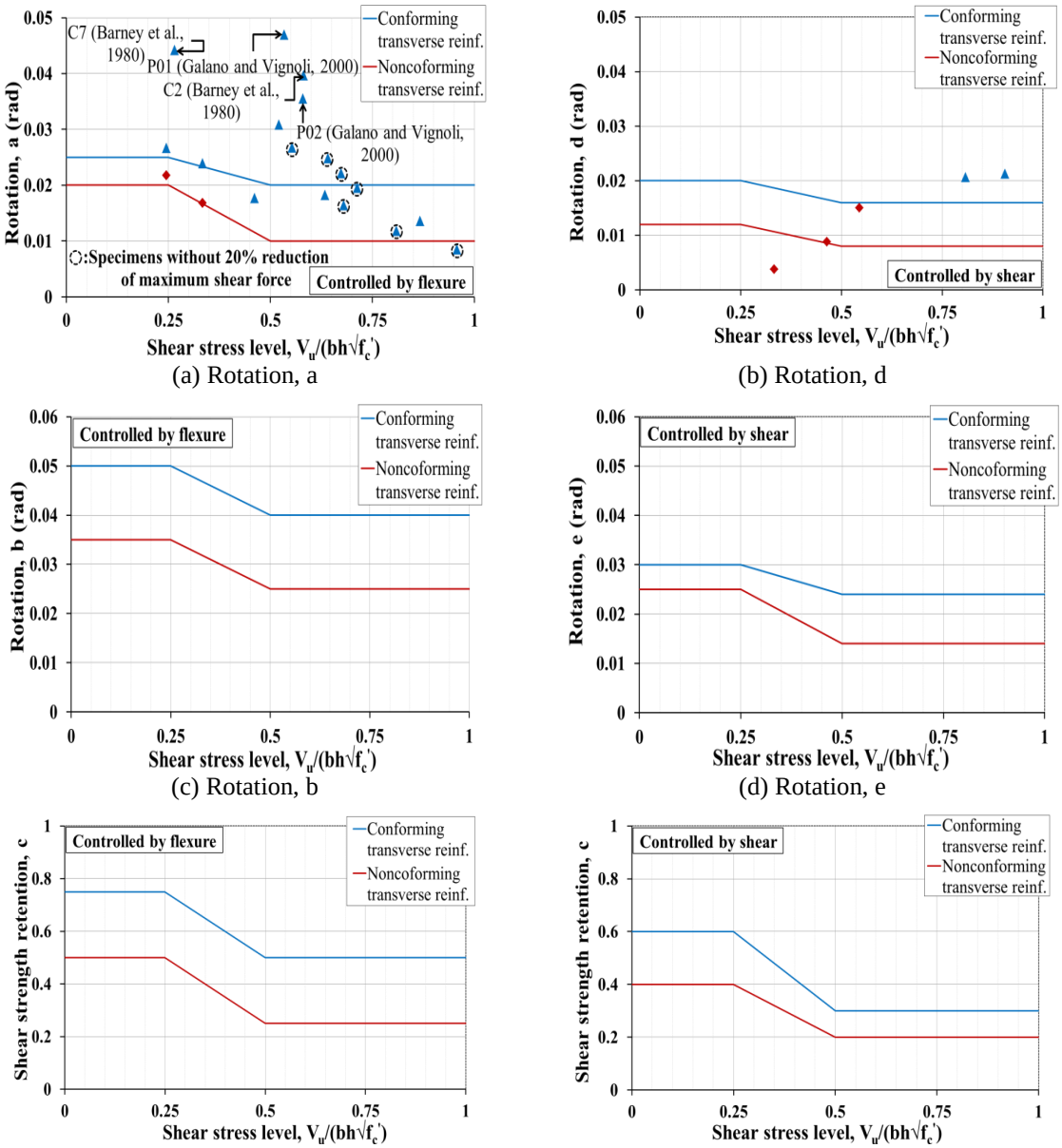

(a) Rotation, a (b) Rotation, d

(c) Rotation, b (d) Rotation, e

(e) Strength retention ratio, c (f) Strength retention ratio, c

Fig. 8 Modeling parameters for CR coupling beams in ASCE 41-13

The modeling parameters specified for CR and DR coupling beams in ASCE 41-13 (Table 1) are examined in comparison with the compiled test results. The experimental values for chord rotations "a" and "d" in Figs. 8 and 9 are determined at the point of a 20% strength drop from the maximum load in the experimental shear-rotation backbone curve. This is based on the common practice that the displacement ductility is defined at

the point of a 20% strength reduction from the peak load (Paulay and Priestley 1992). The experimental value for shear strength retention ratio "c" is calculated as the shear strength at the last drift level divided by the maximum load of the test. The experimental values for chord rotations "a" and "d" are quite scattered mainly due to different transverse reinforcement details and shear stress levels (Figs. 8 and 9).

5.1 Conventionally reinforced (CR) coupling beams

Most CR coupling beams governed by flexure had conforming transverse reinforcement per ASCE 41-13, while two of them (Bristowe 2006) had nonconforming transverse reinforcement, as indicated in Fig. 8. For the CR beams governed by flexure (Fig. 8a), the ASCE 41 modeling values for both cases of transverse reinforcement are conservative compared with the test results on average, although a few specimens with shear stress levels higher than 0.5 exhibited smaller rotation capacities than those specified in ASCE 41-13. The test results demonstrate that the "a" value tends to decrease as the shear stress demand increases; ASCE 41-13 reflects this with two discrete values and linear interpolation between them (Fig. 8). Some CR beams marked by dotted circles present relatively smaller "a" values that are determined using the rotations measured at the ends of the tests. These specimens did not even experience a 20% strength drop of the maximum load by the end of testing (as noted in Fig. 8).

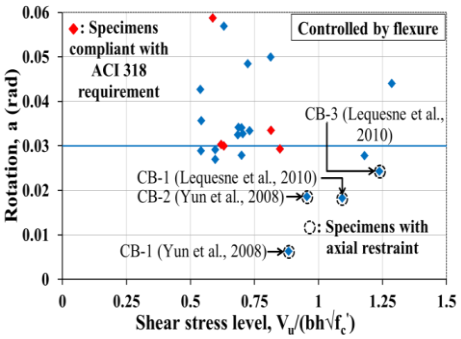

(a) Rotation, a

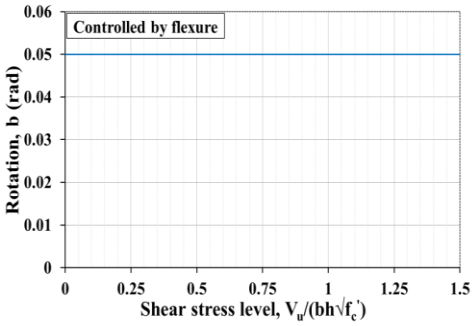

(b) Rotation, b

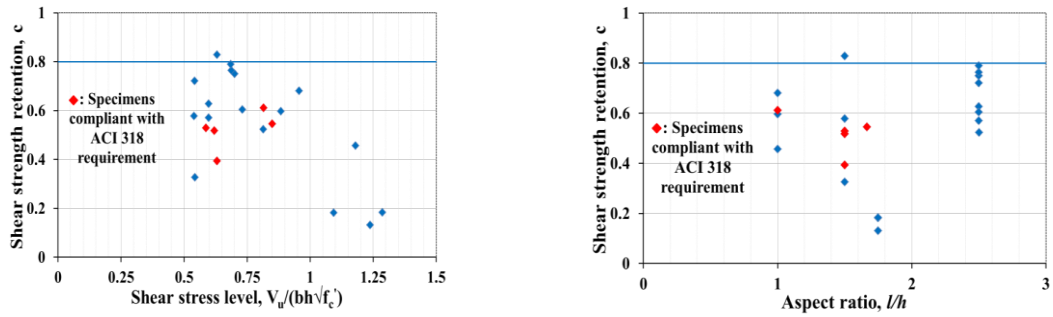

(c) Strength retention ratio

Fig. 9 Modeling parameters for DR coupling beams in ASCE 41-13

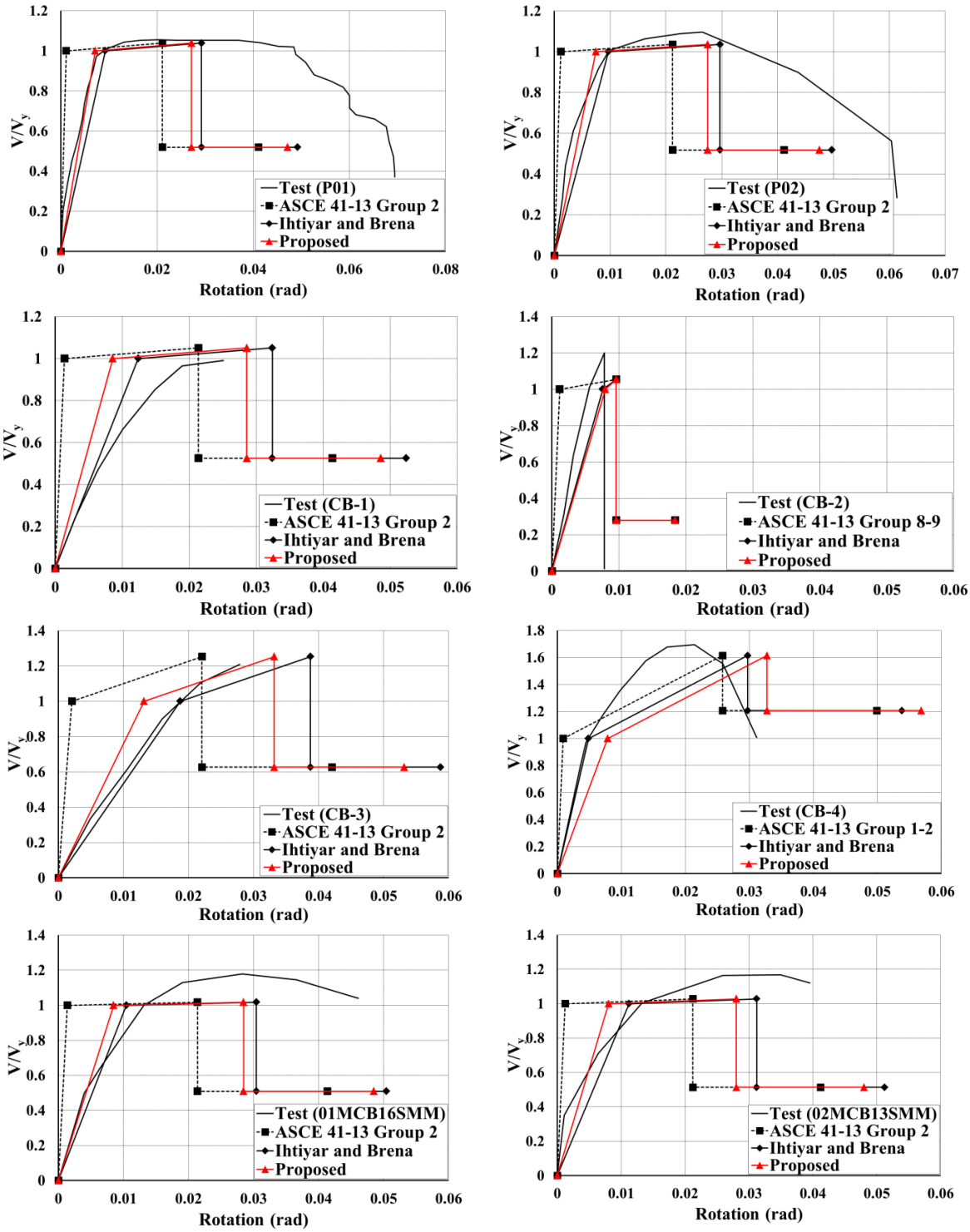

Fig. 10 Calculated vs. tested shear-rotation responses for CR coupling beams

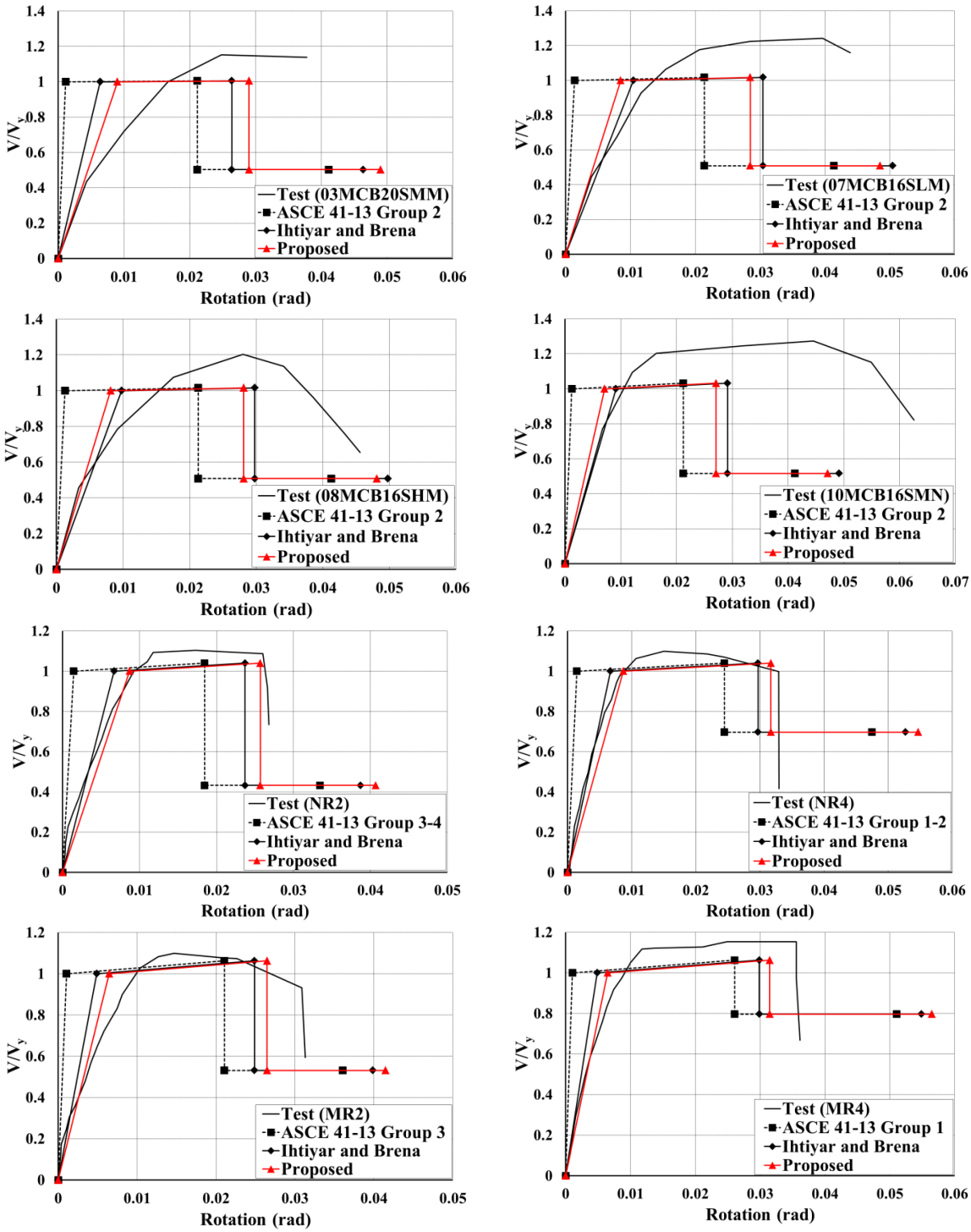

Fig. 10 Calculated vs. tested shear-rotation responses for CR coupling beams (Continued)

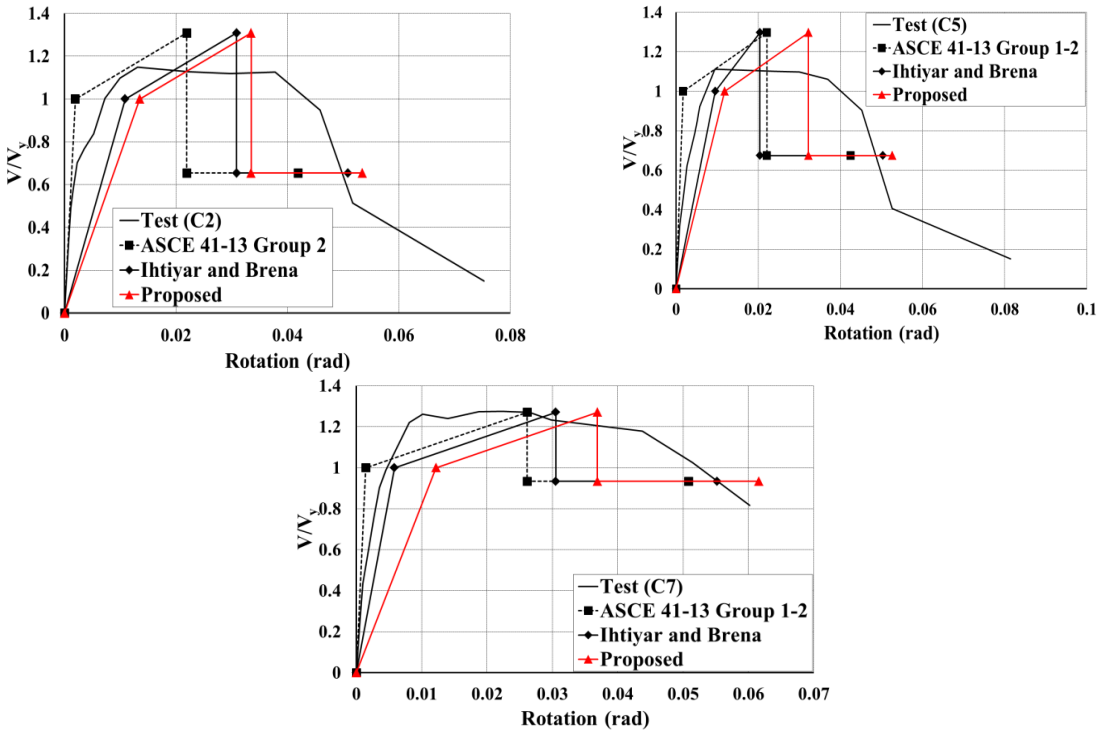

Fig. 10 Calculated vs. tested shear-rotation responses for CR coupling beams (Continued)

For the CR beams governed by shear (Fig. 8b), experimental "d" values are generally in agreement with the ASCE 41 modeling values, although only a small number of specimens are collected for this category (Ihtiyar and Breña 2007, Hong and Jang 2006). The specimens with non-conforming transverse reinforcement exhibited smaller chord rotations than those with conforming transverse reinforcement. However, quantitative evaluations on this category of coupling beams are difficult due to the limited number of specimens. Other modeling rotations "b", "e" and strength retention ratio "c" are also plotted with no experimental data compared.

5.2 Diagonally reinforced coupling beams

For the DR coupling beams in Table 3, the experimental values for chord rotation "a" and strength retention ratio "c" are obtained and compared with the ASCE 41 modeling values in Table 1. It is noted that the DR coupling beams compliant with Section 21.9.7 of ACI 318-11 are expected to show only flexure-controlled behaviors according to ASCE 41-13. The ACI requirements specify minimum four bars of diagonal reinforcement provided in two or more layers, and suitable confinement of the diagonal bar groups provided by both transverse and horizontal reinforcements. In fact, only a few specimens (Tassios *et al*. 1996, Galano and Vignoli 2000) fall into the DR coupling beams compliant with ACI 318-11, as indicated in Fig. 9.

Most experimental "a" values are close to or larger than the ASCE 41 modeling value that is specified 0.03 (Fig. 9a). However, some specimens (Yun *et al*. 2008, Lequesne *et al*. 2010) tested under high shear stress levels and axial restraint present lower rotation capacities, which are

marked by dotted circles in Fig. 9a. It is seen that the experimental "a" value generally gets smaller as the shear stress level increases. However, ASCE 41-13 does not consider the effect of shear stress level on the deformation capacity of DR coupling beams.

The average of all the experimental "c" values plotted in Fig. 9 is about 0.40 (the average of the specimens compliant with ACI 318-11 is about 0.52), which is much smaller than the ASCE 41 modeling value equal to 0.80. This reveals an important point that ASCE 41-13 overestimates the strength retention capacity of DR coupling beams designed following the current codes. Also, in general, the experimental "c" value becomes smaller as the shear stress level increases (Fig. 9c), while the effect of the length-to-depth aspect ratio is not clearly identified (Fig. 9d).

6. Evaluation of coupling beam shear-rotation models

The shear force-chord rotation models reviewed earlier are evaluated based on the compiled test database of CR and DR coupling beams in Tables 2 and 3. The experimental backbone curve of each coupling beam is constructed by capturing successive points in the hysteretic shear-rotation response at different drift levels. Each point corresponds to the peak shear force at each drift level. Three analytical models applied for the CR coupling beams in Fig. 10 are based on ASCE 41-13 (2013), Ihtiyar and Brena (2009), and the proposed yield-stiffness method of this study. The strength of a coupling beam is calculated following the ACI 318 requirements (2011). Once the chord yield-rotation values are determined by the aforesaid analytical models, the other rotation and strength values are calculated using the ASCE 41-13 coefficients presented in Table 1. The schematic backbone model of ASCE 41-13 is shown in Fig. 3. For the DR coupling beams in Fig. 11, the truss model by Hindi and Hassan (2007) is applied additionally.

For classified comparisons, the ASCE modeling parameters for RC coupling beams are categorized into 13 groups as shown in Table 1. The simplified shear-rotation backbone curve of each group of RC coupling beams is illustrated in Fig. 1. Figs. 10 and 11 compare the experimental backbone curves of CR and DR coupling beams with those constructed by the analytical backbone curves, respectively. Unfortunately, unloading branches were not captured during some experiments by the completion of testing. In some specimens, insufficient transverse reinforcement resulted in a brittle failure mode without the yielding of longitudinal reinforcement (Tassios *et al*. 1996, Ihtiyar and Breña 2007, Hong and Jang 2006).

Among the 13 groups per ASCE 41-13, most CR coupling beams fall into Group 2 of which behaviors are dominated by flexure in the presence of conforming transverse reinforcement. The analytical backbone curves per ASCE 41-13 show larger discrepancies from the experimental results, mainly due to the underestimation of chord yield rotations. The discrepancies become smaller by introducing the modified cracked moment of inertia per Ihtiyar and Brena (2007). Furthermore, the chord yield rotations obtained through the proposed yield stiffness method are similar to those by Ihtiyar and Brena (2007). The chord yield rotations per Ihtiyar and Brena's model and the proposed method of the study are about 17.8% and 21.2% larger than those per ASCE 41-13 (2013) on average, respectively.

For the DR coupling beams that are classified as only Group 5, ASCE 41-13 commonly underestimates chord yield rotations compared with the experimental backbone curves. The chord yield rotations estimated by the proposed yield stiffness method are similar to those by Ihtiyar and Brena (2007), which are much closer to the test results than by ASCE 41-13. The truss model by

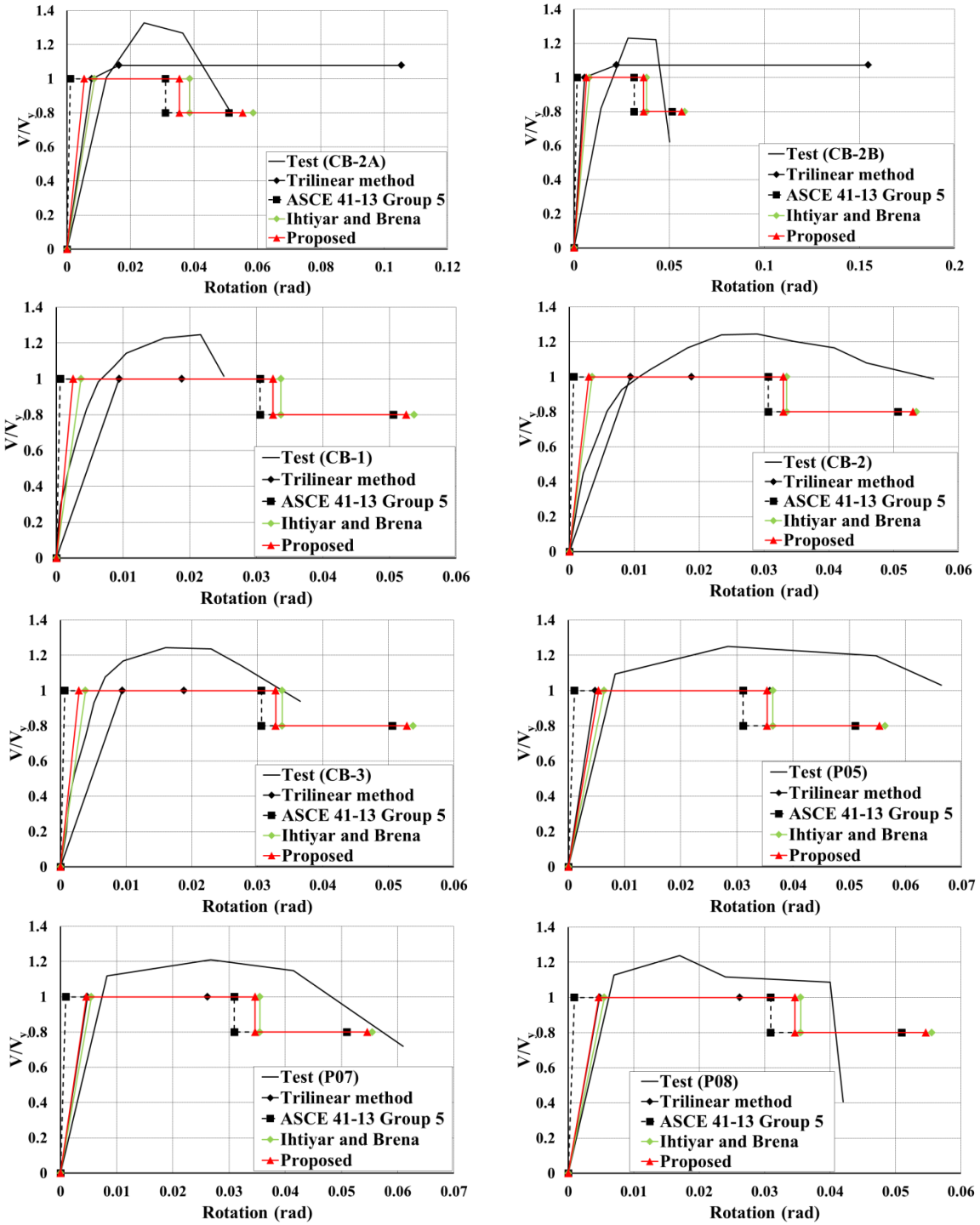

Fig. 11 Calculated vs. tested shear-rotation responses for DR coupling beams

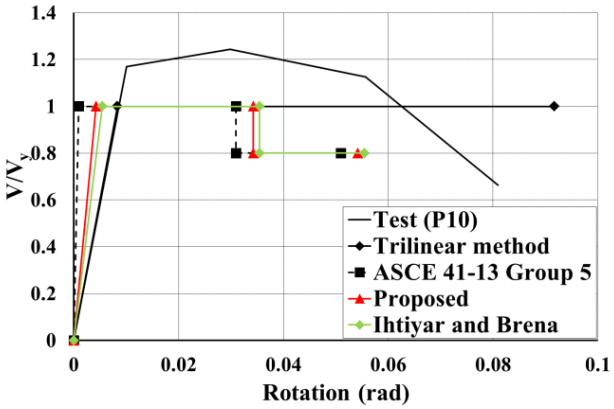

Fig. 11 Calculated vs. tested shear-rotation responses for DR coupling beams (Continued)

Hindi and Hassan (2007) only applied for the DR beams, called "Trilinear method" in Fig. 11, generally produces larger chord yield rotations than the other methods. One limitation of Hindi and Hassan's model is not to consider strength degradation at large rotations. For some specimens Galano and Vignoli (2000), Lequesne *et al*. (2010), bilinear approximations are made due to the absence of adequate concrete confinement in the diagonal elements, so that the 1st and 2nd points in the trilinear curve overlap each other. (An unconfined concrete core does not develop additional compressive stress, and there is no change of strain along the diagonal element).

7. Conclusions

In this study, the reliability of ASCE 41-13 modeling parameters specified for RC coupling beams are assessed based on a database compiling almost all coupling beam tests available worldwide. Several recently developed coupling beam models are also reviewed, and a rational method is proposed for determining the chord yield rotation of RC coupling beams. Important findings and conclusions are summarized in the following:

1. ASCE 41-13 generally underestimates the chord yield rotation of RC coupling beams compared with the test results.
2. Using the modified cracked moment of inertia, Ihtiyar and Brena (2007) suggested taking into account reinforcing bar slippage at the coupling beam-wall interfaces. The chord yield rotations estimated per this model are greatly closer to the test results than than those per ASCE 41-13.
3. The yield stiffness method proposed in this study predicts similar chord yield rotations to those by Ihtiyar and Brena's model.
4. For the CR coupling beams, the test results suggest that the rotation parameters "a" and "d" specified in ASCE 41-13 appear to be reasonable.
5. For the DR coupling beams, the rotation parameter "a" given in ASCE 41-13 is conservative compared with the test results in general. However, ASCE 41-13 does not consider the negative effect of shear stress level on the deformation capacity of DR coupling beams.
6. ASCE 41-13 greatly overestimates the strength retention capacity of DR coupling beams designed following the current codes.

Acknowledgments

This research was supported by Basic Science Research Program through the National Research Foundation of Korea (NRF) funded by the Ministry of Education, Science and Technology (Grant No. 2010-0022955). Also, support from Global Ph.D. Fellowship Program through the National Research Foundation of Korea (NRF) funded by the Ministry of Education (NRF-2014H1A2A1020435) is acknowledged.

References

ACI Committee 318 (2011), Building code requirements for structural concrete (318-11) and commentary (318R-11), American Concrete Institute, Farmington Hills, MI, USA.

ICC (2012), International building code, International Code Council, Washington, DC, USA.

Technical Committee CEN/TC 250 (2004), Eurocode 8: Design of structures for earthquake resistance – Part 1: General rules, seismic actions and rules for buildings. European Committee for Standardization, Brussels, Belgium.

Canadian Standards Association (2010), CAN/CSA A23.3-04: Design of concrete structures. Canadian Standards Association, Mississauga, Ontario, Canada.

New Zealand Standards Council (2006), NZS 3101-1: Concrete structures standard – The design of concrete structures. Standards New Zealand, Wellington, New Zealand.

Paulay, T. and Priestley, M.J.N. (1992), Seismic design of reinforced concrete and masonry structures. John Wiley & Sons, New York, NY, USA.

Paulay, T. (1971), "Coupling beams of reinforced concrete shear walls", *J. Struct. Div.*, **97**(3), 843-862.

Tassios, T.P., Moretti, M. and Bezas, A. (1996), "On the behavior and ductility of reinforced concrete coupling beams of shear walls", *ACI Struct. J.*, **93**(6), 711-720.

Galano, L. and Vignoli, A. (2000), "Seismic behavior of short coupling beams with different reinforcement layouts", *ACI Struct. J.*, **97**(6), 876-885.

Yun, H.D., Kim, S.W., Jeon, E., Park, W.S. and Lee, Y.T. (2008), "Effects of fibre-reinforced cement composites' ductility on the seismic performance of short coupling beams", *Mag. Concrete Res.*, **60**(3), 223-233.

ASCE (2010), Minimum design loads for building and other structures (ASCE/SEI 7-10). American Society of Civil Engineers, Reston, VA, USA.

ASCE (2013), Seismic rehabilitation of existing buildings (ASCE/SEI 41-13), American Society of Civil Engineers, Reston, VA, USA.

ACI Committee 369 (2011), Guide for seismic rehabilitation of existing concrete frame buildings and commentary (ACI 369R-11), American Concrete Institute, Farmington Hills, MI, USA.

Ihtiyar, O. and Breña, S.F. (2006), Force-deformation response of conventionally reinforced coupling beams: evaluation of FEMA 356 and FEMA 306. 8th National Conference on Earthquake Engineering.

Ihtiyar, O. and Breña, S.F. (2007), Assessment of FEMA 356 techniques for orthogonally reinforced coupling beams through experimental testing. ASCE Structures Congress: Structural Engineering Research Frontiers.

Brena, S.F., Fernández Ruiz, M., Kostic, N. and Muttoni, A. (2009), Modelling techniques to capture the backbone envelope behaviour of coupling beams subjected to seismic loading. Studi e ricerche, Starrylink, 29 (EPFL-ARTICLE-143412).

Barney, G.B. (1980), Behavior of coupling beams under load reversals. Portland Cement Association, Skokie, IL, USA.

Bristowe, S. (2006), Seismic response of normal and high strength concrete members, PhD Thesis, McGill University, Montreal, Canada.

Hong, S.G. and Jang, S.K. (2006), "The mechanism of load resistance and deformability of reinforced concrete coupling beams", *J. Earthq. Eng.Soc. Korea*, **10**(3), 113-123.

Paulay, T. and Binney, J.R. (1974), Diagonally reinforced coupling beams of shear walls. Shear in reinforced concrete, SP-42, American Concrete Institute, Farmington Hills, MI, USA, 579-598.

Lequesne, R., Setkit, M., Parra-Montesinos, G.J. and Wight, J.K. (2010), Seismic detailing and behavior of coupling beams with high-performance fiber-reinforced concrete. SP-271, American Concrete Institute, Farmington Hills, MI, USA, 189-204.

Canbolat, B.A., Parra-Montesinos, G.J. and Wight, J.K. (2005), "Experimental study on seismic behavior of high-performance fiber-reinforced cement composite coupling beams", *ACI Struct. J.*, **102**(1), 159-166.

Shimazaki, K. (2004), De-bonded diagonally reinforced beam for good repairability. 13th World Conference on Earthquake Engineering, Paper No. 3173.

Hindi, R. and Hassan, M. (2007), "Simplified trilinear behavior of diagonally reinforced coupling beams", *ACI Struct. J.*, **104**(2), 199-206.

Mander, J.B., Priestley, M. J. and Park, R. (1988), "Theoretical stress-strain model for confined concrete", *J. Struct. Eng.*, **114**(8), 1804-1826.

Shin, M., Gwon, S.W., Lee, K., Han, S.W. and Jo, Y.W. (2014), "Effectiveness of high performance fiber-reinforced cement composites in slender coupling beams", *Construct. Build. Mater.*, **68**, 476-490.

Wallace, J.W. (2007), "Modelling issues for tall reinforced concrete core wall buildings", *Struct. Des. Tall Special Build.*, **16**(5), 615-632.

Cowper, G.R. (1966), "The shear coefficient in Timoshenko's beam theory", *J. Appl.Mech.*, **33**(2), 335-340.

FEMA (2000), *Prestandard and commentary for the seismic rehabilitation of buildings (FEMA 356)*, Federal Emergency Management Agency, Washington, DC, USA.

Naish, D., Fry, A., Klemencic, R. and Wallace, J. (2013), "Reinforced concrete coupling beams—part II: modeling", ACI Struct. J., **110**(06), 1067-1075.

Wallace, J.W. (2012), "Behavior, design, and modeling of structural walls and coupling beams – lessons from recent laboratory tests and earthquakes. International Journal of concrete structures and materials", **6**(1), 3-18.

Kim, I.H., Sun, C.H. and Shin, M. (2012), "Concrete contribution to initial shear strength of RC hollow bridge columns", *Struct. Eng. Mech.*, **41**(1), 43-65.